Precise Measurement of the Neutron Magnetic Form Factor

G.P.Gilfoyle, J.D.Lachniet, W.K.Brooks, M.F.Vineyard, B.Quinn (the E5 group),*

and the CLAS Collaboration

Outline:
1. Motivation.
2. Background.
3. Measuring G_M^n.
4. Results and Systematic Uncertainties.
5. Impact and Conclusions.

* Thesis project.

Scientific Motivation

- The neutron magnetic form factor $G_M^n(Q^2)$ is a fundamental observable related to the spatial distribution of the charge and magnetization in the neutron.

Scientific Motivation

- The neutron magnetic form factor $G_M^n(Q^2)$ is a fundamental observable related to the spatial distribution of the charge and magnetization in the neutron.
- Part of a broad effort to answer the question ‘What is the internal landscape of the nucleons?’.*

* ‘The Frontiers of Nuclear Science: A Long-Range Plan’, NSF/DOE Nuclear Science Advisory Committee, December, 2007.

Scientific Motivation

- The neutron magnetic form factor $G_M^n(Q^2)$ is a fundamental observable related to the spatial distribution of the charge and magnetization in the neutron.
- Part of a broad effort to answer the question ‘What is the internal landscape of the nucleons?’.*
- The elastic electromagnetic form factors (EEFFs) G_M^n, G_E^n, G_M^p, and G_E^p constrain the generalized parton distributions (GPDs) which promise to give us a three-dimensional picture of hadrons.

$*$ ‘The Frontiers of Nuclear Science: A Long-Range Plan’, NSF/DOE Nuclear Science Advisory Committee, December, 2007.

Scientific Motivation

- The neutron magnetic form factor $G_M^n(Q^2)$ is a fundamental observable related to the spatial distribution of the charge and magnetization in the neutron.
- Part of a broad effort to answer the question 'What is the internal landscape of the nucleons?'.*
- The elastic electromagnetic form factors (EEFFs) G_M^n, G_E^n, G_M^p, and G_E^p constrain the generalized parton distributions (GPDs) which promise to give us a three-dimensional picture of hadrons.
- EEFFs are a fundamental and early challenge for lattice QCD.

* 'The Frontiers of Nuclear Science: A Long-Range Plan', NSF/DOE Nuclear Science Advisory Committee, December, 2007.

Scientific Motivation

- The neutron magnetic form factor $G_M^n(Q^2)$ is a fundamental observable related to the spatial distribution of the charge and magnetization in the neutron.
- Part of a broad effort to answer the question 'What is the internal landscape of the nucleons?'.*
- The elastic electromagnetic form factors (EEFFs) G_M^n, G_E^n, G_M^p, and G_E^p constrain the generalized parton distributions (GPDs) which promise to give us a three-dimensional picture of hadrons.
- EEFFs are a fundamental and early challenge for lattice QCD.

We present new data with precision and coverage that eclipse the world's data in this Q^2 range.

* 'The Frontiers of Nuclear Science: A Long-Range Plan', NSF/DOE Nuclear Science Advisory Committee, December, 2007.

Some Necessary Background

- For convenience use the Sachs form factors to express the cross section for elastic scattering.

$$\frac{d\sigma}{d\Omega} = \sigma_{Mott}\left(\frac{(G_E^n)^2 + \tau(G_M^n)^2}{1+\tau} + 2\tau\tan^2\frac{\theta}{2}(G_M^n)^2\right)$$

where E (E') is the incoming (outgoing) electron energy, θ is the scattered electron angle, $\tau = \frac{Q^2}{4M^2}$, and $\sigma_{Mott} = \frac{\alpha^2 E' \cos^2(\frac{\theta}{2})}{4E^3\sin^4(\frac{\theta}{2})}$.

- At low momentum transfer ($Q^2 \ll M_N^2$) G_E and G_M are the Fourier transforms of the densities of charge and magnetization. At high Q^2 relativistic effects make the interpretation more interesting!

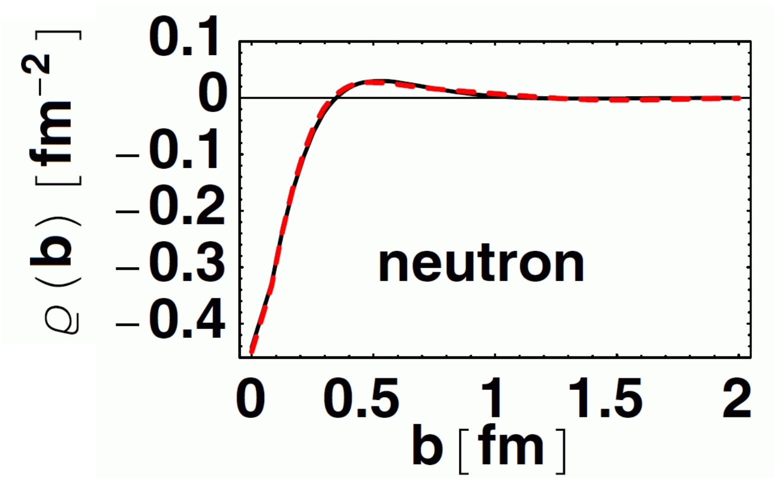

G.A.Miller, Phys.Rev.Lett.99:112001,2007

Current World Data on EEFFs

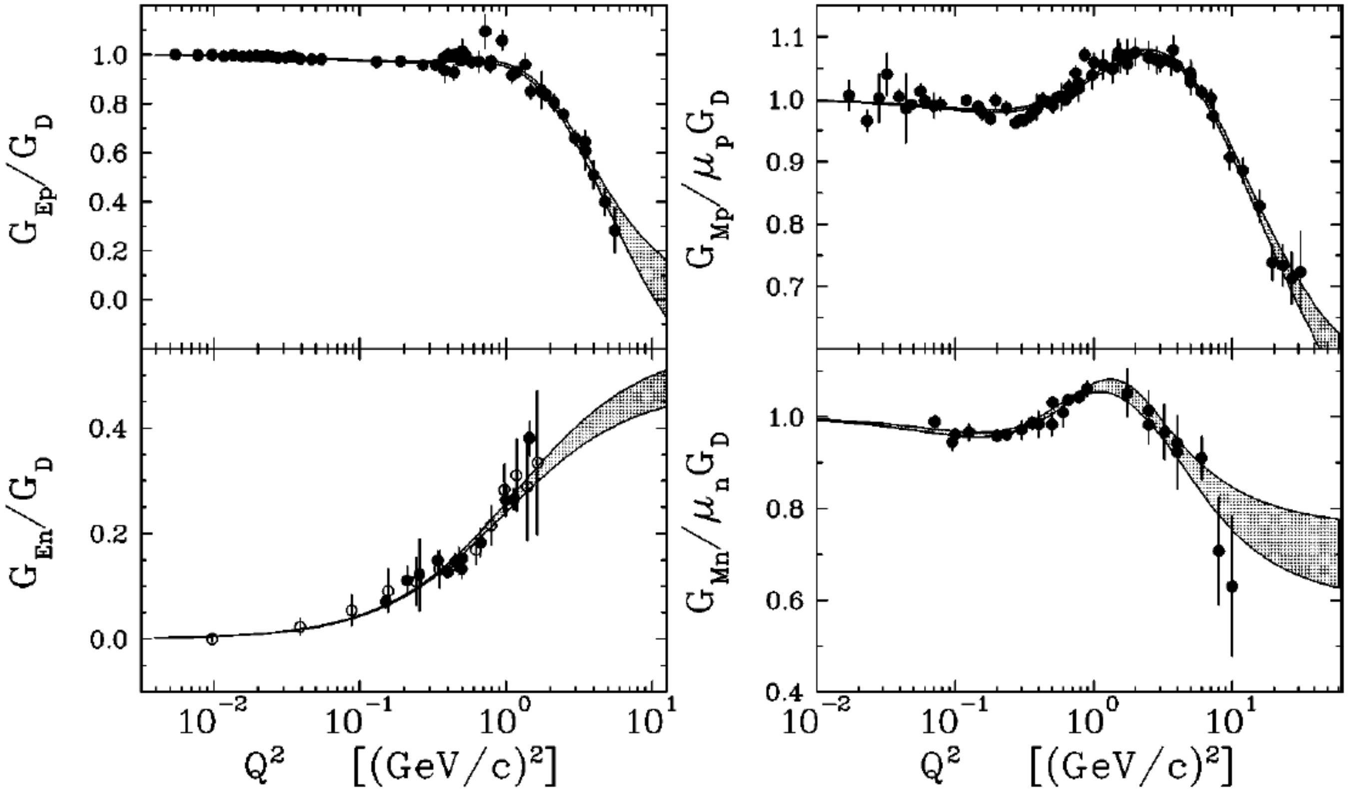

J.J.Kelly, Phys. Rev.C, 068202, 2004.

- Proton form factors have small uncertainties and reach higher Q^2.
- Neutron form factors are sparse and have large uncertainties.
- Significant deviations from the dipole form factor.

The Experiment- Jefferson Lab

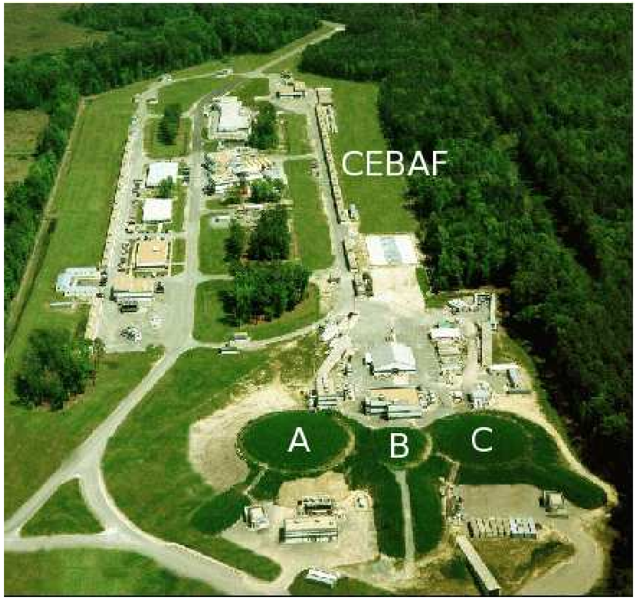

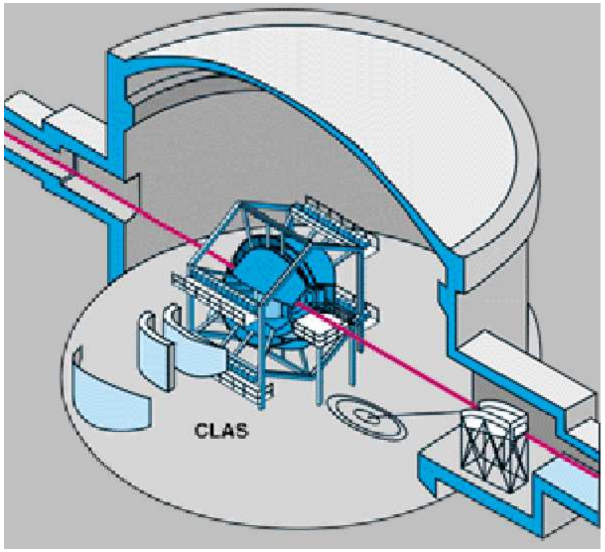

Continuous Electron Beam Accelerator Facility (CEBAF)

- Superconducting Electron Accelerator (338 cavities), 100% duty cycle.
- $E_{max} = 6$ GeV, $\Delta E/E = 10^{-4}$, $I_{max} = 200\ \mu A$, $P_e \geq 80\%$.

Hall B - CEBAF Large Acceptance Spectrometer (CLAS)

- Nearly 4π-acceptance spectrometer with a toroidal magnet ($\Delta p/p = 0.5\%$, $\mathcal{L} \approx 10^{34}\ cm^{-2}s^{-1}$).
- Layers of drift chambers, Cherenkov counters, time-of-flight (TOF) scintillators, and electromagnetic calorimeter (EC).
- Neutrons detected in both TOF and EC.
- Dual, collinear target with liquid hydrogen and deuterium.
- E5 data set: 4.2 GeV and 2.6 GeV; 2.3 billion triggers.

Measuring G_M^n - The Ratio Method

- Without a free neutron target we use deuterium and measure R

$$R = \frac{\frac{d\sigma}{d\Omega}[^2\mathrm{H}(e,e'n)_{QE}]}{\frac{d\sigma}{d\Omega}[^2\mathrm{H}(e,e'p)_{QE}]}$$

$$= a(E, Q^2, \theta_{pq}^{max}, W^2_{max}) \times \frac{\sigma_{Mott}\left(\frac{(G_E^n)^2+\tau(G_M^n)^2}{1+\tau} + 2\tau\tan^2\frac{\theta}{2}(G_M^n)^2\right)}{\frac{d\sigma}{d\Omega}[^1\mathrm{H}(e,e')p]}$$

  where $a(E, Q^2, \theta_{pq}^{max}, W^2_{max})$ corrects for nuclear effects, θ_{pq}^{max} and W^2_{max} are kinematic cuts, and the numerator is the precisely-known proton cross section.

- Less vulnerable to nuclear structure (*e.g.*, deuteron model, *etc.*) and experimental effects (*e.g.*, electron acceptance, *etc.*).
- Must accurately measure the nucleon detection efficiencies and match the geometric solid angles.

The Ratio Method - Selecting Quasielastic Events

- Kinematic definitions.
- $e-n/e-p$ selection: standard criteria for electrons and protons; TOF and calorimeter (EC) are TWO, INDEPENDENT neutron measurements.
- Quasi-elastic event selection: Apply a maximum θ_{pq} cut to eliminate inelastic events plus a cut on W^2 (L. Durand, Phys. Rev. 115, 1020 (1959)).
- Acceptance matching: Use the quasi-elastic electron kinematics to predict if the nucleon (proton or neutron) lies in CLAS acceptance. Require both hypotheses to be satisfied.

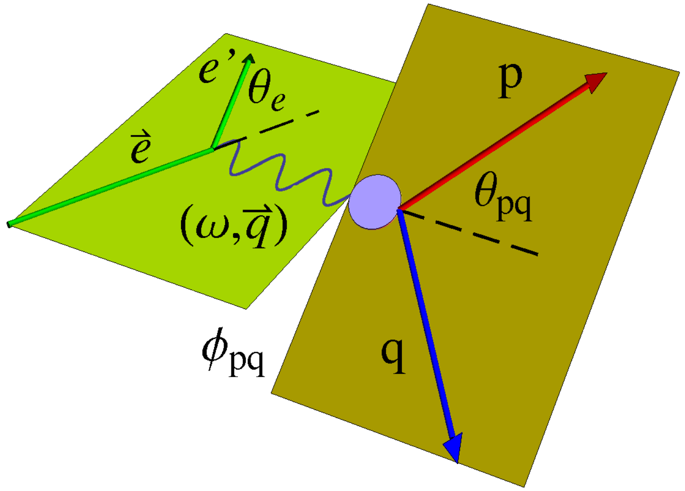

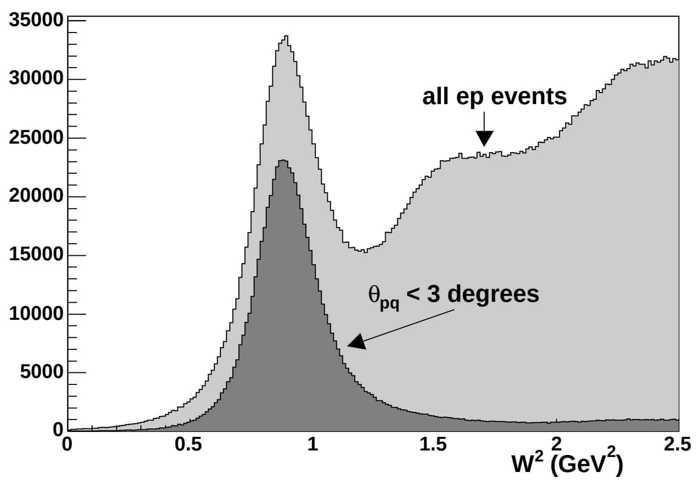

Neutron/Proton Detection Efficiencies

1. Use dual target cell for *in situ* calibrations.
2. Make tagged neutrons with $ep \to e'\pi^+ n$ from the $^1\mathrm{H}$ target. In the EC and TOF use the missing momentum to predict the neutron location and search for it.
3. Use $ep \to e'p$ elastic scattering for tagged protons. In the TOF use the missing momentum from $ep \to e'X$ to predict the proton location and search that paddle or an adjacent one.

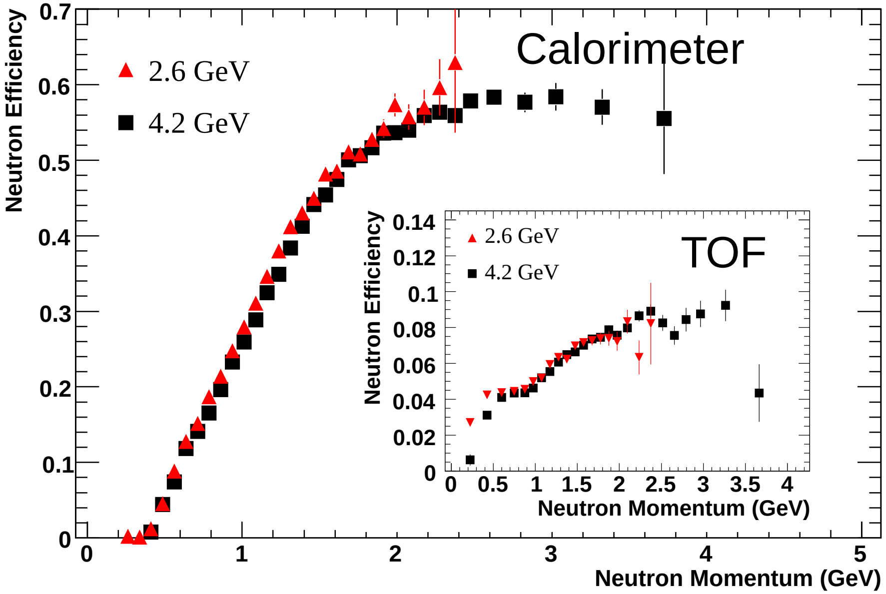

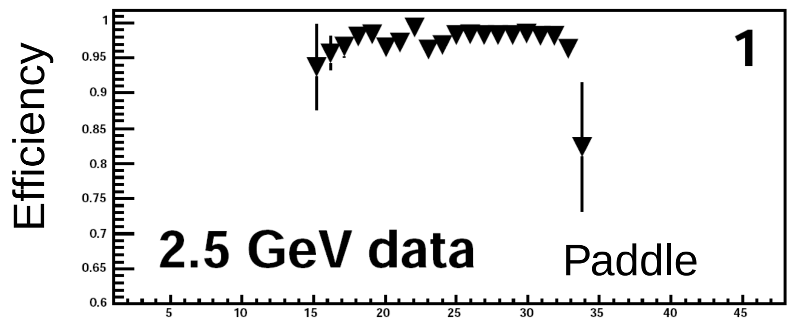

Systematic Uncertainties

Quantity	2.6 GeV (%)	4.2 GeV (%)	Quantity	2.6 GeV (%)	4.2 GeV (%)
Calorimeter neutron efficiency parameterization	< 1.5	< 1.0	TOF neutron efficiency parameterization	< 2.0	< 3.2
proton σ	< 1.0	< 1.5	G_E^n	< 0.5	< 0.7
Fermi loss correction	< 0.8	< 0.9	θ_{pq} cut	< 0.4	< 1.0
neutron accidentals	< 0.07	< 0.3	neutron MM cut	< 0.5	< 0.07
neutron proximity cut	< 0.22	< 0.15	proton efficiency	< 0.3	< 0.35
Nuclear Corrections	< 0.17	< 0.2	Radiative corrections	< 0.05	< 0.06

Upper limits on percent estimated systematic uncertainty for different contributions.

Goal: Systematic uncertainty less than 3% on G_M^n.

Results - Overlaps and Final Averages

- The ratio R for each beam energy is the weighted average of the EC and TOF measurements.
- Overlapping measurements of reduced G_M^n are consistent.
- Systematic uncertainty $\frac{\delta G_M^n}{G_M^n} \times 100 < 2.5\%$.

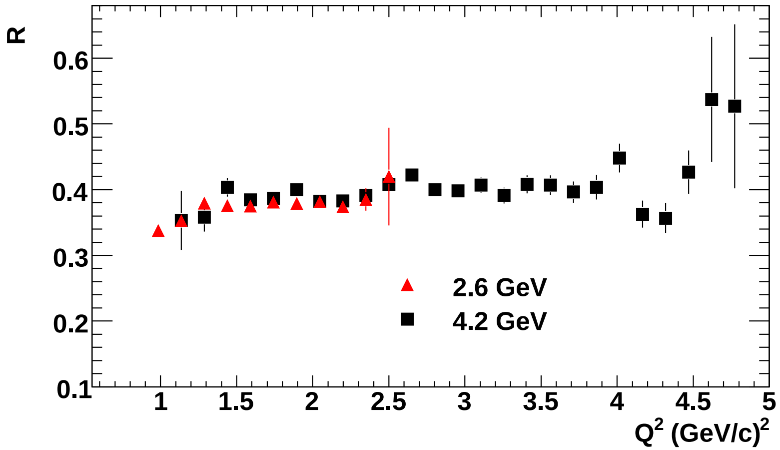

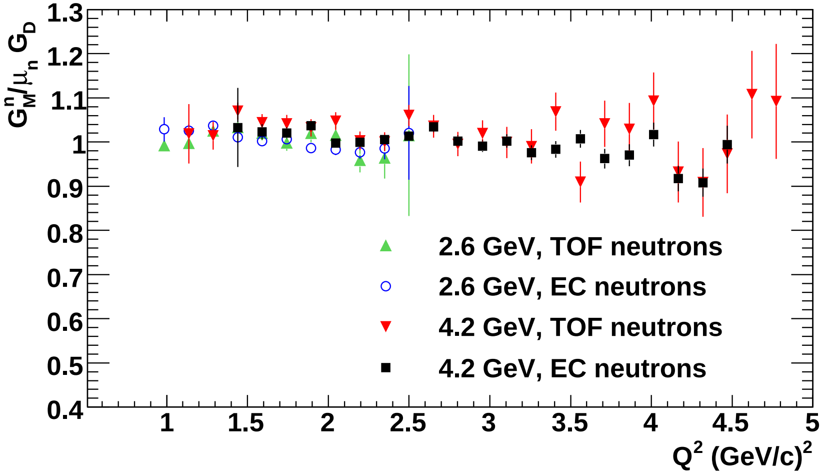

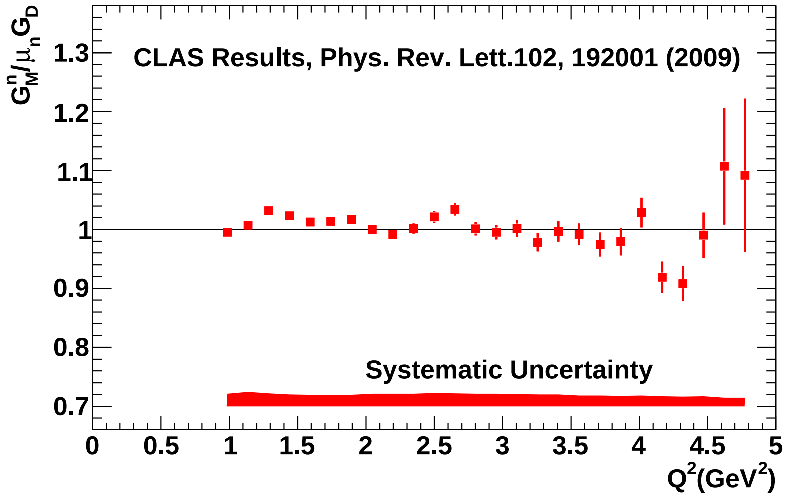

Comparison with Theory

- Green band - Diehl *et al.* (Eur. Phys. J. C 39, 1, 2005) use parameterized GPDs fitted to the data.
- Dashed curve - Guidal *et al.* (Phys. Rev. D 72, 054013, 2005) use a Regge parameterization of the GPDs to describe the elastic nucleon form factors at low Q^2 and extend it to higher Q^2.

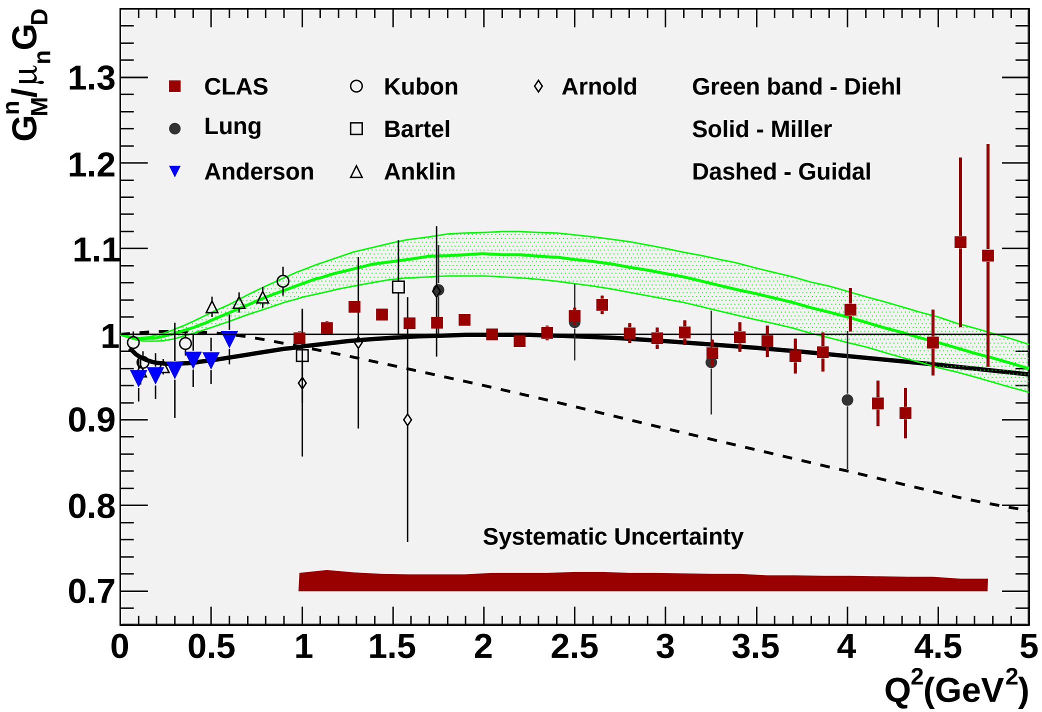

- Black curve - Miller's (Phys. Rev. C 66, 032201(R), 2002) uses light-front dynamics to describe a relativistic system of three bound quarks and a surrounding pion cloud.

Impact on World's Data for G_M^n

- Parameterization of world's data on G_M^n done by J.Kelly (PRC, 70, 068202, 2004) using the following function.

$$\frac{G_M^n}{\mu_n G_D} = \frac{\sum_{k=0}^{n} a_k \tau^k}{1 + \sum_{k=1}^{n+2} b_k \tau^k}$$

$$\tau = \frac{Q^2}{4M_p^2}$$

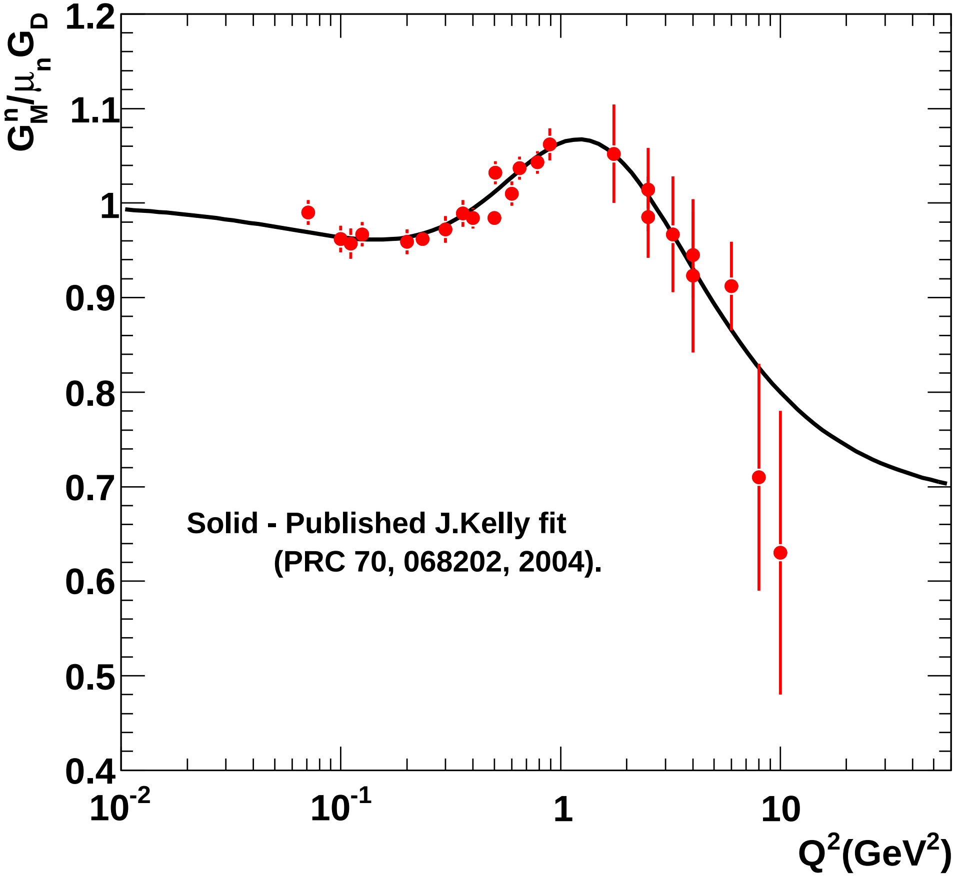

Impact on World's Data for G_M^n

- Parameterization of world's data on G_M^n done by J.Kelly (PRC, 70, 068202, 2004) using the following function.

$$\frac{G_M^n}{\mu_n G_D} = \frac{\sum_{k=0}^{n} a_k \tau^k}{1 + \sum_{k=1}^{n+2} b_k \tau^k}$$

$$\tau = \frac{Q^2}{4M_p^2}$$

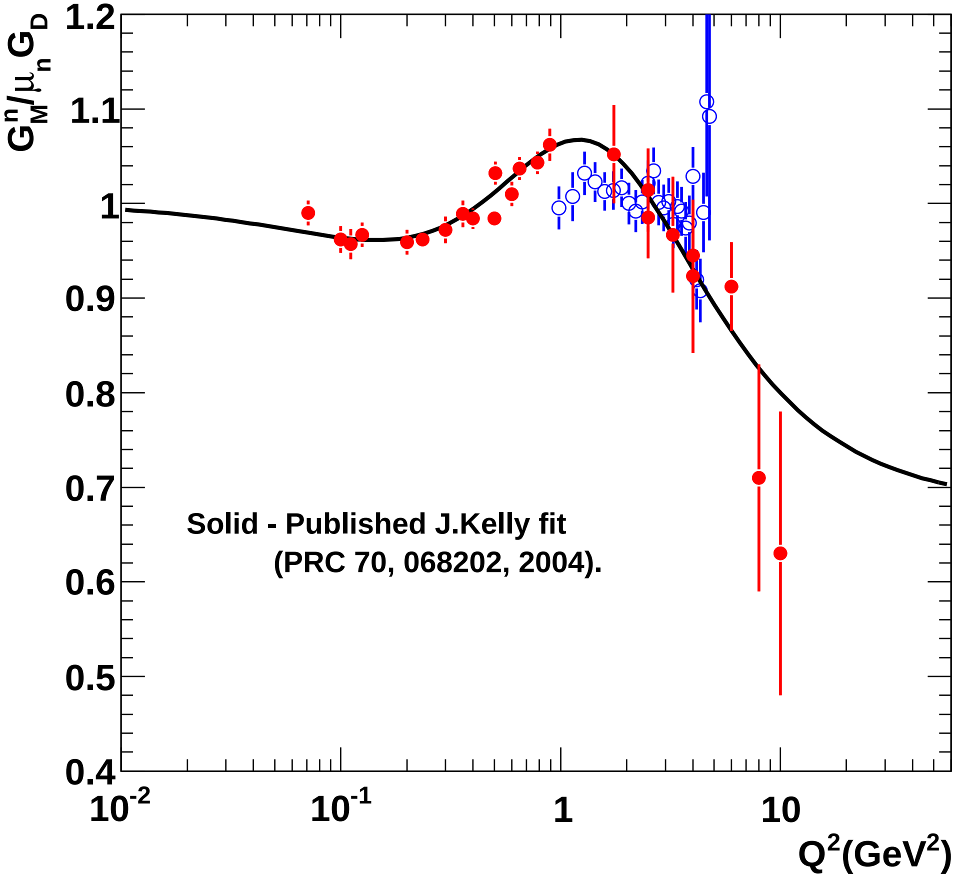

Impact on World's Data for G_M^n

- Parameterization of world's data on G_M^n done by J.Kelly (PRC, 70, 068202, 2004) using the following function.

$$\frac{G_M^n}{\mu_n G_D} = \frac{\sum_{k=0}^{n} a_k \tau^k}{1 + \sum_{k=1}^{n+2} b_k \tau^k}$$

$$\tau = \frac{Q^2}{4M_p^2}$$

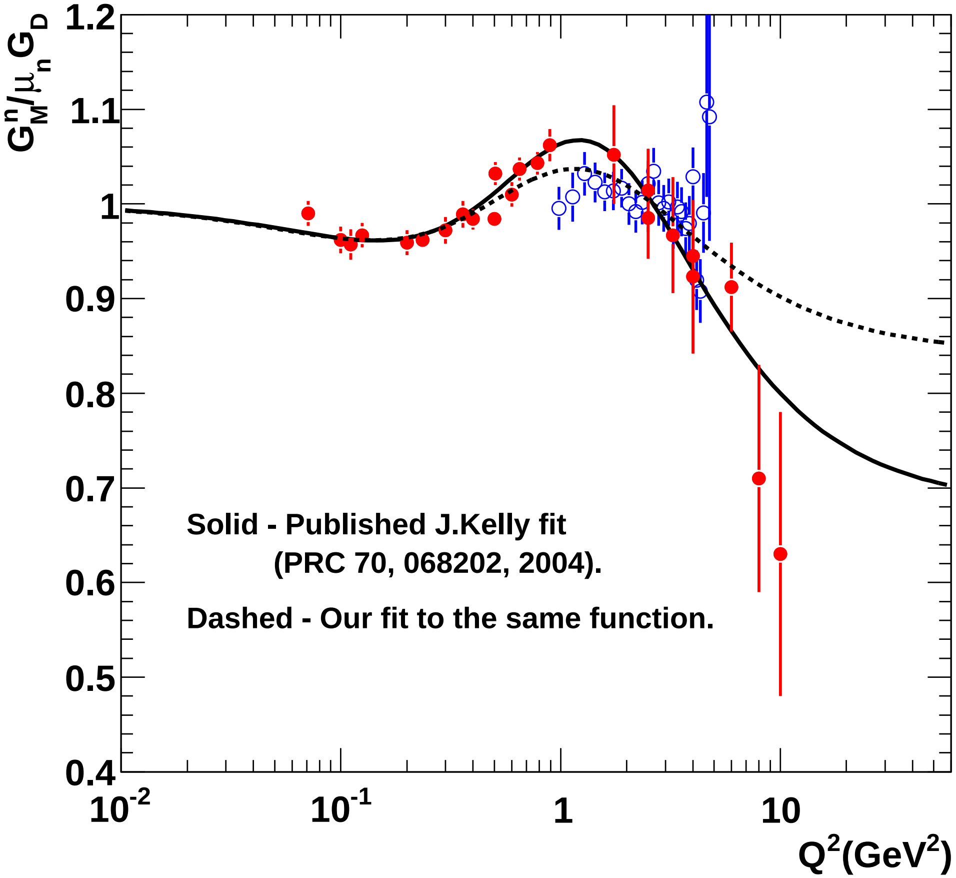

Impact on World's Data for G_M^n

- Parameterization of world's data on G_M^n done by J.Kelly (PRC, 70, 068202, 2004) using the following function.

$$\frac{G_M^n}{\mu_n G_D} = \frac{\sum_{k=0}^{n} a_k \tau^k}{1 + \sum_{k=1}^{n+2} b_k \tau^k}$$

$$\tau = \frac{Q^2}{4M_p^2}$$

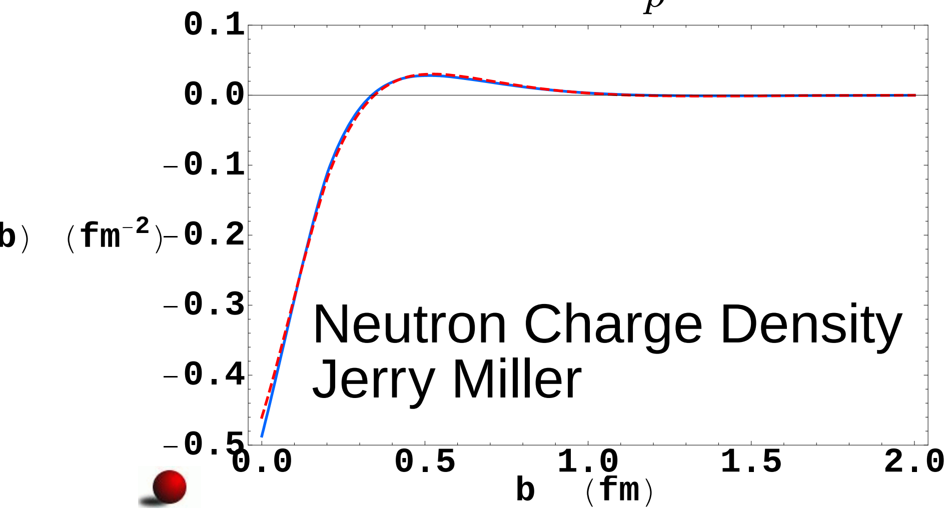

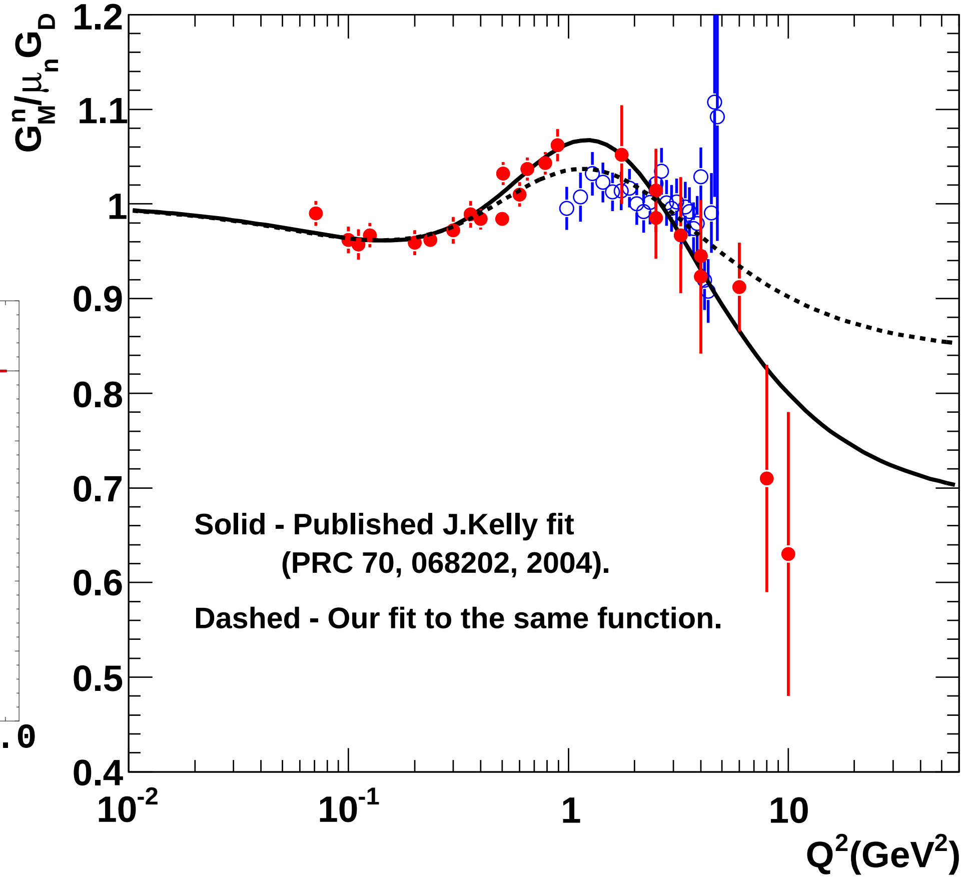

Conclusions

- We have measured the neutron magnetic form factor G_M^n over the range $\mathrm{Q}^2 = 1.0 - 4.8\ (\mathrm{GeV/c})^2$ to a precision better than 2.5%.
- The four different measurements of G_M^n at two beam energies with the calorimeter and the TOF system in CLAS are consistent with each other and with previous results in this Q^2 range.
- The results are consistent with the dipole approximation within 5% across almost the full range of Q^2; differing from many expectations.
- Light-cone calculation by Miller gives the best description of the full G_M^n data set.
- Kelly parameterization of G_M^n changes significantly with the new CLAS data. but this difference has surprisingly little effect on the neutron charge distribution extracted by Jerry Miller.

Conclusions

- We have measured the neutron magnetic form factor G_M^n over the range $\mathrm{Q}^2 = 1.0 - 4.8\ (\mathrm{GeV/c})^2$ to a precision better than 2.5%.
- The four different measurements of G_M^n at two beam energies with the calorimeter and the TOF system in CLAS are consistent with each other and with previous results in this Q^2 range.
- The results are consistent with the dipole approximation within 5% across almost the full range of Q^2; differing from many expectations.
- Light-cone calculation by Miller gives the best description of the full G_M^n data set.
- Kelly parameterization of G_M^n cha … w CLAS data. but this difference ha … e neutron charge distribution extra…
- The future is bright. →

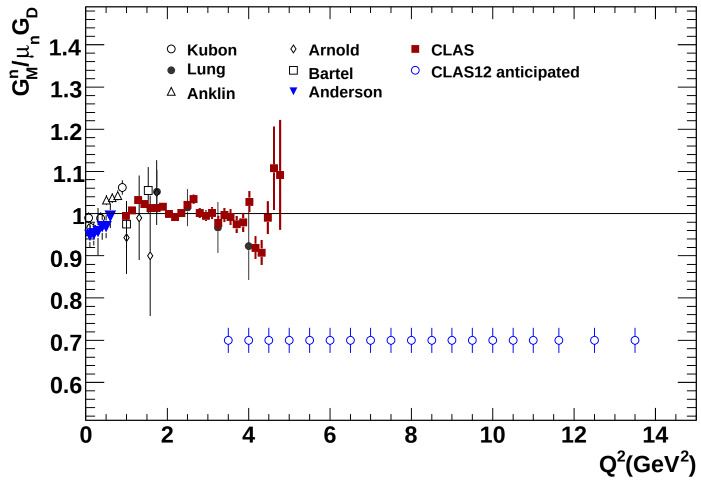

Additional Slides

Experimental Details - E5 Data Set

- Data Set:
  - 2.3 billion triggers.
  - $\mathrm{E} = 4.2\ \mathrm{GeV}$ and $2.6\ \mathrm{GeV}$ with positive torus polarity (electrons inbending).
  - $\mathrm{E} = 2.6\ \mathrm{GeV}$ with negative torus polarity (electrons outbending).
- Dual target cell with liquid hydrogen and deuterium separated by 4.7-cm. Perform *in situ* calibrations during data collection.
- Targets are well separated.

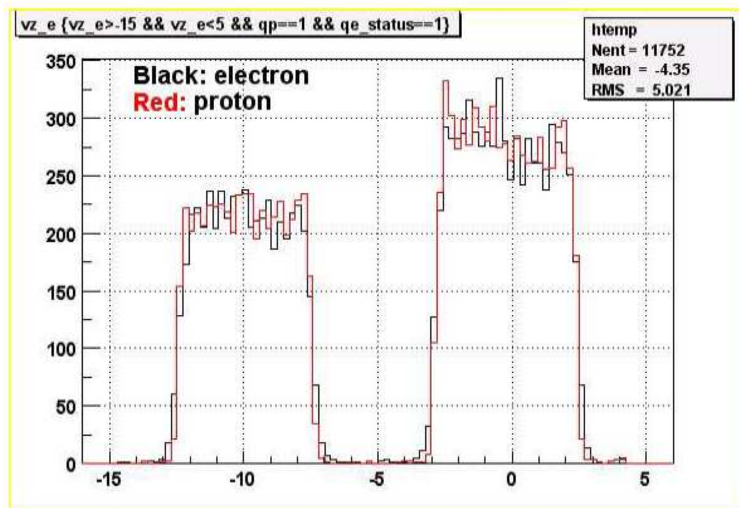

Additional Corrections

- Nuclear effects: The $e-n/e-p$ ratio for free nucleons differs from the one for bound nucleons. Recall the factor $a(E, Q^2, \theta_{pq}^{max}, W_{max}^2)$ in R. Calculations by Jeschonnek and Arenhövel were close to unity.
- Radiative corrections: Calculated for exclusive $D(e, e'p)n$ with the code EXCLURAD (CLAS-Note 2005-022 and PRD, 66, 074004, 2002). Ratio close to unity.
- Fermi motion in the target: Causes nucleons to migrate out of the CLAS acceptance. Effect was simulated to determine correction.
- Momentum corrections.
- Effect of θ_{pq}^{max}.

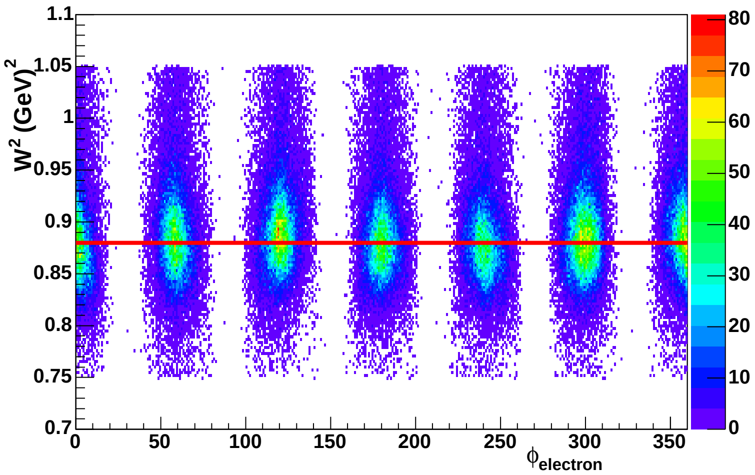

Systematic Uncertainties - NDE

- Calorimeter neutron detection efficiency (NDE) parameterization:
  1. NDE fitted with a third order polynomial plus a flat region at higher momentum.
  2. Highest order term was dropped and the ratio R regenerated.
  3. The upper limit on the range of values of R extracted from the different NDE fits was assigned as the systematic uncertainty.
- TOF NDE parameterization: Similar to calorimeter extraction except the second and third order terms in the polynomial were dropped.
- These are the largest contributions from this measurement.

Detector	2.6 GeV	4.2 GeV
Calorimeter	<1.5	<1.0
TOF	<2.0	<3.2

Percentage systematic uncertainties in neutron detection efficiency parameterization.

Lomon Calculations

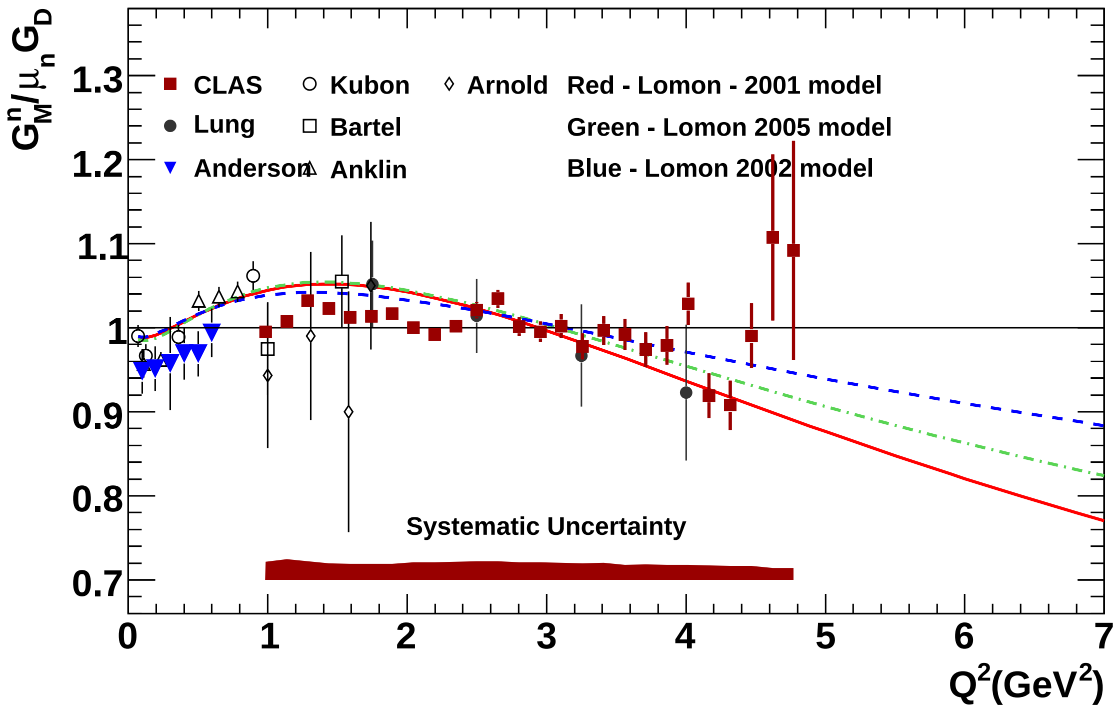

- 2001 Model - Used dcs(?) (Rosenbluth) data for G_E^n and G_E^p and no polarization data.
- 2005 Model - Gives same result for G_M^n as 2008 model which included low Q^2 $R_n = \mu_n G_E^p / G_M^n$ and $R_p = \mu_p G_E^n / G_M^n$ results from BLAST and preliminary, high-Q^2 results for R_n from JLab.
- 2002 Model

Anklin *et al.* and Kubon *et al.* Measurements

- Used the ratio method to measure G_M^n.
- Neutrons detected in scintillator array consisting of thick E and thin ΔE counters.
- Protons detected in same scintillator array using the energy TOF and the E signals.
- Neutron detection efficiency measurement performed at the Paul Scherrer Institute.
  - High (low) energy neutron beam produced in the $^{12}\mathrm{C}(\mathrm{p,n})$ ($\mathrm{D}(\mathrm{p,n})$) reaction and then scattered off a liquid H_2 target.
  - Neutrons scattering off the liquid H_2 target were tagged by detecting the recoil proton from the $\mathrm{H}(\mathrm{n,p})\mathrm{n}$ reaction.
  - Final sample of tagged neutrons used to measure NDE.

Experimental Details - EC NDE Difference

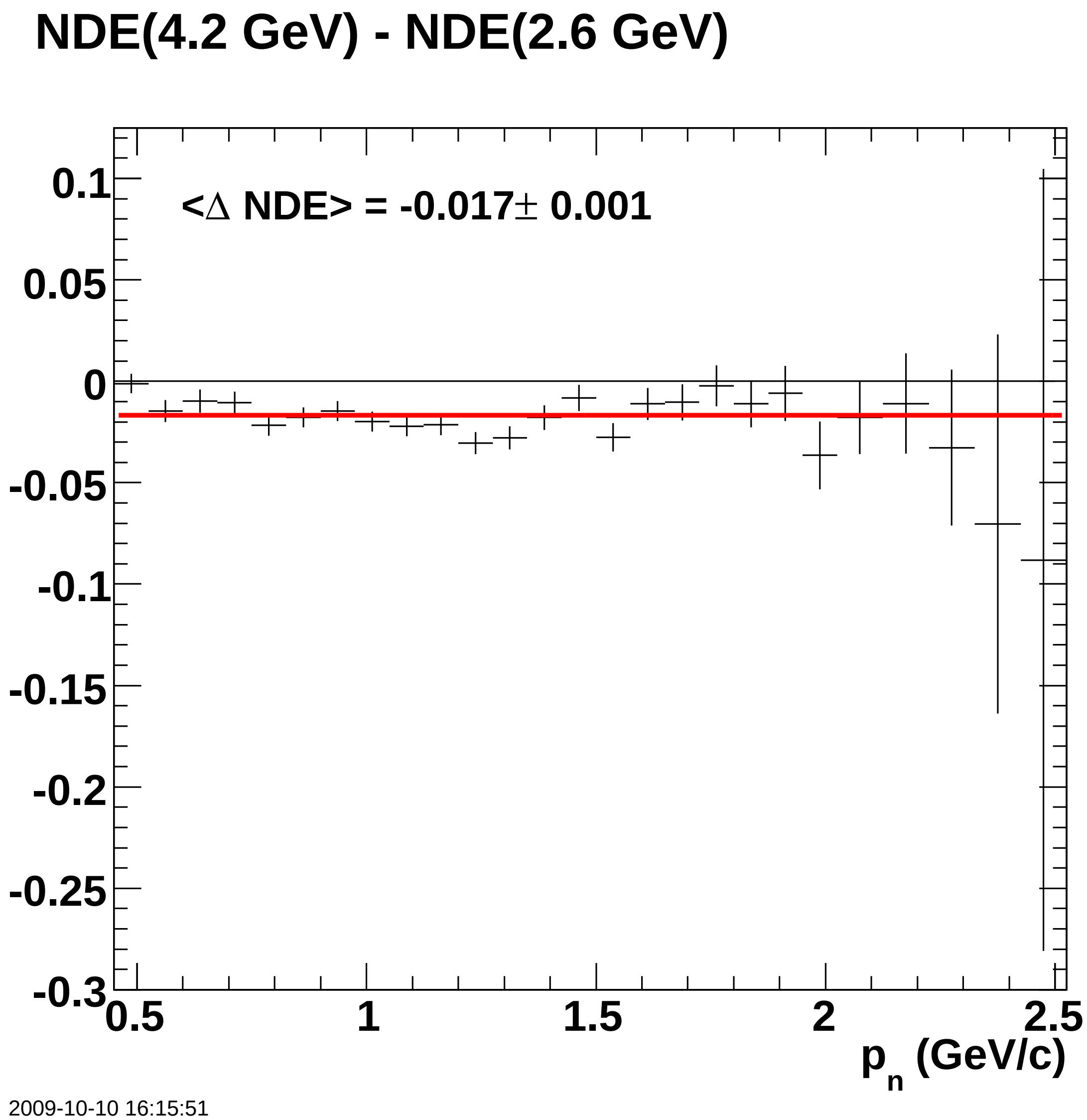

G_E^n/G_M^n

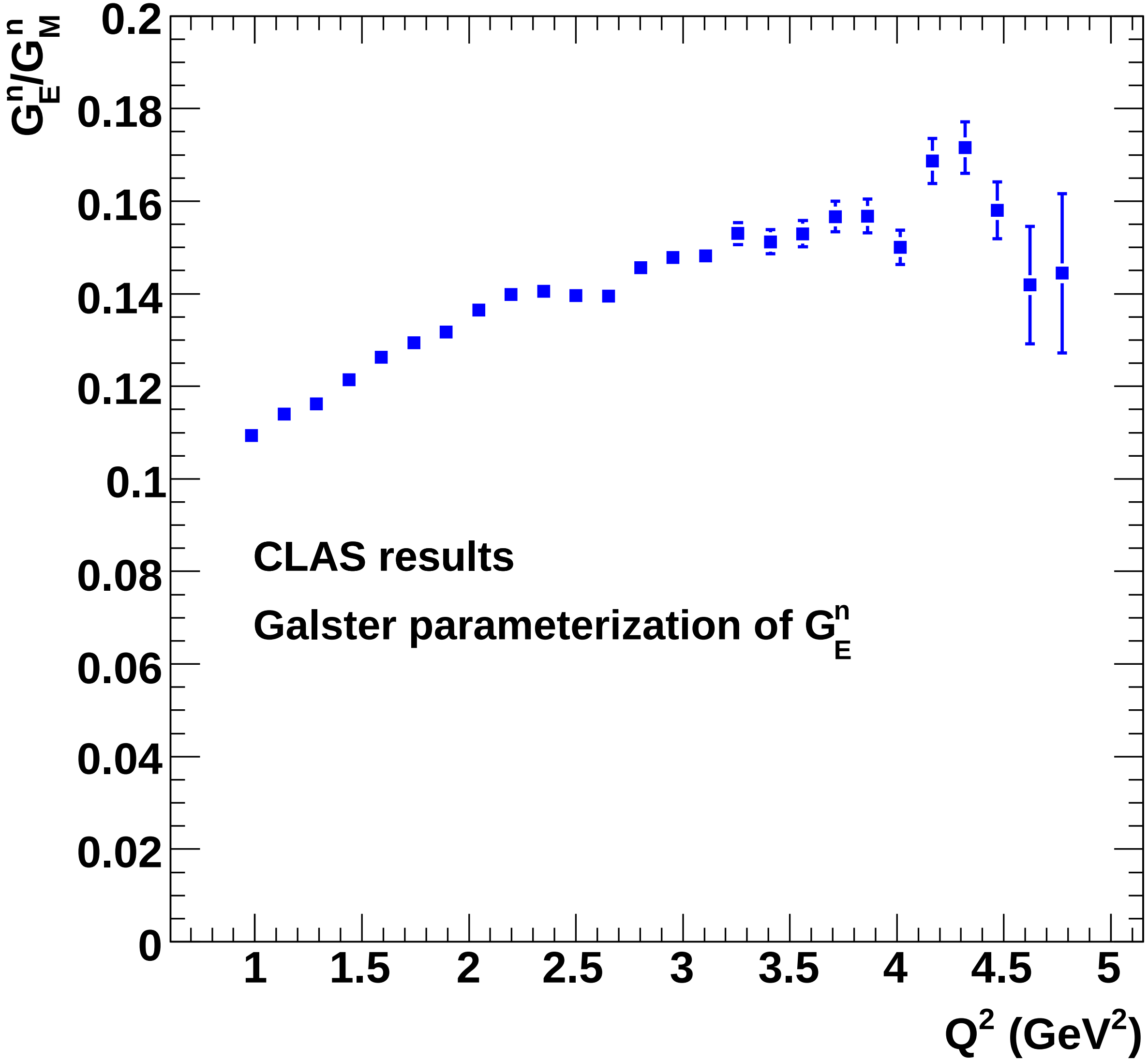

G_E^n/G_M^n
0.2
0.18
0.16
0.14
0.12
0.1
0.08
0.06
0.04
0.02
0
1
1.5
2
2.5
3
3.5
4
4.5
5
Q^2 (GeV^2)
CLAS results
Galster parameterization of G_E^n

Effect of Fermi Correction

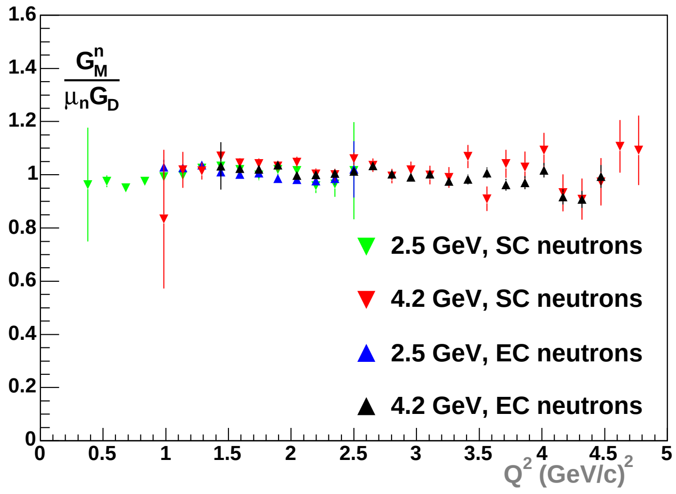

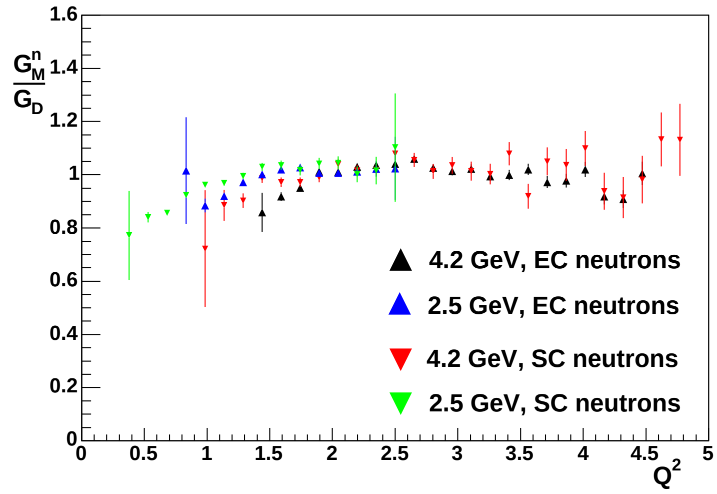

Reduced G_M^n for four different measurements.

Reduced G_M^n for four different measurements. The Fermi corrections have not been applied.